Non-Covalent Interactions

Deutsche Ausgabe: DOI: 10.1002/ange.201503905
Internationale Ausgabe: DOI: 10.1002/anie.201503905

Aromatic Gain in a Supramolecular Polymer**

*Victorio Saez Talens, Pablo Englebienne, Thuat T. Trinh, Willem E. M. Noteborn, Ilja K. Voets, and Roxanne E. Kieltyka**

Abstract: *The synergy of aromatic gain and hydrogen bonding in a supramolecular polymer is explored. Partially aromatic bis(squaramide) bolaamphiphiles were designed to self-assemble through a combination of hydrophobic, hydrogen-bonding, and aromatic effects into stiff, high-aspect-ratio fibers. UV and IR spectroscopy show electron delocalization and geometric changes within the squaramide ring indicative of strong hydrogen bonding and aromatic gain of the monomer units. The aromatic contribution to the interaction energy was further supported computationally by nucleus-independent chemical shift (NICS) and harmonic oscillator model of aromaticity (HOMA) indices, demonstrating greater aromatic character upon polymerization: at least 30% in a pentamer. The aromatic gain–hydrogen bonding synergy results in a significant increase in thermodynamic stability and a striking difference in aggregate morphology of the bis(squaramide) bolamphiphile compared to isosteres that cannot engage in this effect.*

Aromatic gain is considered to be a thermodynamic driving force in several organic reactions. In aromatic substitutions, Bergman cyclizations, aromatic Cope rearrangements, [1,5]H sigmatropic shifts, and [4+2] cyclizations, among others, the restoration of aromaticity helps to explain their exergonic character and increased efficiency.[1] In supramolecular polymers,[2] where monomers are held together by non-covalent interactions resulting in higher-order aggregates with various topologies, the concept of aromatic gain in the construction of such systems is unexplored.

Aromaticity has captivated chemists since its introduction as a concept 150 years ago by Kekulé.[3] In contrast to other chemical concepts, such as chemical bonding, electronegativity and acidity/basicity, aromaticity is not a direct physical observable and its exact definition is the subject of much debate.[4] Classically, cyclic π-conjugated compounds are aromatic when they show differences in geometric, energetic, and magnetic criteria relative to their acyclic analogues.[5] In recent years, computational methods such as nucleus-independent chemical shift (NICS),[5c,6] harmonic oscillator model of aromaticity (HOMA),[7] and aromatic stabilization energies (ASE),[5b] have grown in use to describe aromaticity. In the case of NICS, excellent correlation has been reported with experimental nuclear magnetic resonance data as well as other descriptors of aromaticity,[4a] thus opening the door to predict the aromaticity of new compounds and structures a priori. Very recently, NICS calculations demonstrated reciprocal hydrogen-bonding–aromaticity relationships that can have important consequences on the strength of hydrogen-bonding interactions.[8]

Squaramides,[9] which are composed of two NH hydrogen-bond donors opposite two carbonyl hydrogen-bond acceptors on a conformationally rigid cyclobutene ring, are predicted to show partial aromatic character.[9] This character arises from the delocalization of the nitrogen lone pair into the cyclobutenedione ring system (Hückel's rule: $(4n+2)$ π electrons, $n=0$).[10] In the solid state, catemers of disecondary squaramides arranged in a head-to-tail motif have been reported[11] and they may benefit from strong resonance-assisted hydrogen bonding (RAHB) interactions similar to squaric acids.[12] Applications of the squaramide unit have been found in medicinal chemistry, catalysis, and anion recognition.[13] The capacity of squaramides to form strong hydrogen bonds that simultaneously influence their aromatic character is highly appealing to guide the formation of increasingly stable supramolecular polymers. Herein, we incorporate the squaramide synthon into a bolaamphiphilic construct that self-assembles into stiff fibers in water, and we explore the coupling of hydrogen-bonding and aromatic gain using experiment and computation.

Compound **1** consists of two oligo(ethylene glycol) methyl ether chains opposite a central hydrophobic core with two embedded squaramide units (Figure 1). ^{1}H NMR spectra of **1** in D_2O were suggestive of strong aggregation that is resistant to thermal denaturation up to 65 °C. Only ^{1}H NMR spectra recorded in $CDCl_3$ or [D_2]HFIP were well-resolved and suggestive of various degrees of depolymerization.

The effect of the squaramide synthon on the self-assembly of **1** in water was evaluated by cryo-transmission electron

[*] V. Saez Talens, W. E. M. Noteborn, Dr. R. E. Kieltyka
Department of Supramolecular and Biomaterials Chemistry
Leiden Institute of Chemistry, Leiden University
P.O. Box 9502, 2300 RA Leiden (The Netherlands)
E-mail: r.e.kieltyka@chem.leidenuniv.nl
Dr. P. Englebienne
Process & Energy Laboratory
Delft University of Technology
Leeghwaterstraat 39, 2628 CB Delft (The Netherlands)
Dr. T. T. Trinh
Department of Chemistry
Norwegian University of Science and Technology
7491 Trondheim (Norway)
Dr. I. K. Voets
Department of Chemical Engineering and Chemistry and
Institute for Complex Molecular Systems
Eindhoven University of Technology
P.O. Box 513, 5600 MB Eindhoven (The Netherlands)

[**] We thank R.I. Koning (TEM), B. Koster (TEM), F. Galli (AFM), M. Rabe (IR), A. J. M. Sweere (CULGI), R. Matadeen (TEM, NeCEN), K. Pieterse (ICMS Animation Studio), and A. Kros for essential discussions. This work is funded by a VENI grant (to R.E.K.) from NWO.

Supporting information for this article is available on the WWW under http://dx.doi.org/10.1002/anie.201503905.

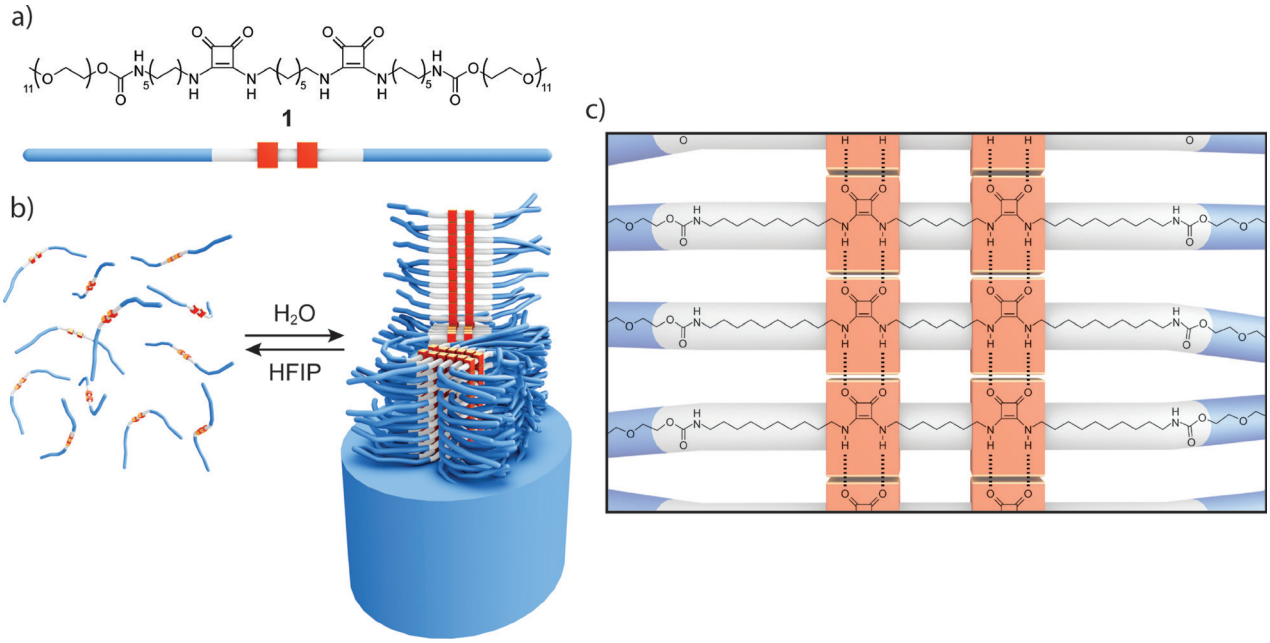

Figure 1. a) Structure of the squaramide-based bolaamphiphile **1**. b) Self-assembly of **1** into fibrillar structures, and depolymerization by hexafluoroisopropanol (HFIP). Within the fibrillar structure, hydrogen bonds are proposed to occur parallel to the fiber axis while π-interactions between squaramide bolaamphphiles occur in the lateral direction, as depicted. c) Proposed hydrogen-bonding interactions between squaramide monomers.

microscopy (cryo-TEM) and atomic force microscopy (AFM). Cryo-TEM images of **1** (1 wt %) displayed stiff, micrometer-long fibrils with a uniform diameter. Short, rod-like structures on the order of 12.6 ± 2.4 nm in length were found upon sonication (Figure 2a) and slowly progressed into micrometer-long fibers. Fibers of **1** were 6.4 ± 1.2 nm in diameter, on par with the length of the hydrophobic region of the bolaamphiphile (Figure 2b). By small-angle X-ray scattering measurements (SAXS, Figure 2c), a cross-sectional radius (r_{cs}) of 3.5 nm and a cross-sectional mass per unit length (M_L) of 2.5×10^{20}–6.0×10^{20} g nm^{-1} was determined for fibers of **1**, indicating that approximately 10–30 squaramide bolaamphiphiles per nm can be found along the fiber axis. These results suggest that hydrogen bonds parallel to the fiber axis drive the formation of highly anisotropic fibers, meanwhile the combination of hydrophobic and π-interactions between squaramide moieties facilitate the assembly of several bolaamphiphiles in the lateral direction (Figure 1).

To better understand the consequence of self-assembly on the squaramide synthon, spectroscopy at the molecular level was pursued. UV spectroscopy of **1** in water showed maxima at 255 and 329 nm, and a shoulder around 310 nm (Figure 3a). Disruption of the polymerized state was achieved using both temperature and various solvents. More specifically, hexafluoroisopropanol (HFIP), a potent hydrogen bond disruptor, promoted depolymerization resulting in the gradual loss of the red-shifted hydrogen-bonded squaramide N–H proton-donor π–π* bands (329 nm) and the blue-shifted C=O proton-acceptor n–π* bands (255 nm), concomitant with the growth of the non-hydrogen bonded monomer band (310 nm).[14] These experimental trends are in agreement with TD-DFT calculations, where two superimposed absorption bands of similar intensity corresponding to the HOMO–LUMO and HOMO–(LUMO + 1) transitions are predicted for the monomer; in oligomers, the high wavelength band is progressively red-shifted while the other appears blue-shifted. Self-assembly of **1** through strong hydrogen bonding interactions results in increased orbital overlap between squaramide units and further electron delocalization within the individual squaramide rings, enabling aromatic gain to occur.

Geometric changes to the squaramides upon self-assembly were examined by IR spectroscopy. Solutions of **1** (2 wt %) in D_2O were measured at room temperature. Above the amide I region, a small broad band at 1796 cm^{-1}, consistent with squaramide ring breathing, was found experimentally and confirmed by modeling (Figure 3b). In the amide I region, asymmetric and symmetric C=O stretches (1687, 1676, and 1642 cm^{-1}) of the squaramide and carbamate moieties were recorded. Strong hydrogen bonding of the squaramide units was observed through the N–H stretch at 3162 cm^{-1} (inset in Figure 3b). In [D_2]HFIP, the blue-shifting of several bands such as the ring breathing (13 cm^{-1}) and symmetric C=O stretch (14 cm^{-1}) modes were observed and suggestive of depolymerization. Owing to lack of transparency of [D_2]HFIP in the N–H region, an approximation for free N–H stretch (3452 cm^{-1}) was made for **1** in $CDCl_3$. The experimental data correlated well with ab initio calculations. These results revealed that bond lengths in the squaramide are systematically altered as a function of oligomer length (Figure 4a): double bonds become longer, whereas single bonds shorten, resulting in a ring with less bond length alternation. With these bond lengths, we computed HOMA values of −0.015 and 0.516 for the isolated monomer and the central monomer in a pentamer, respectively, while a value of

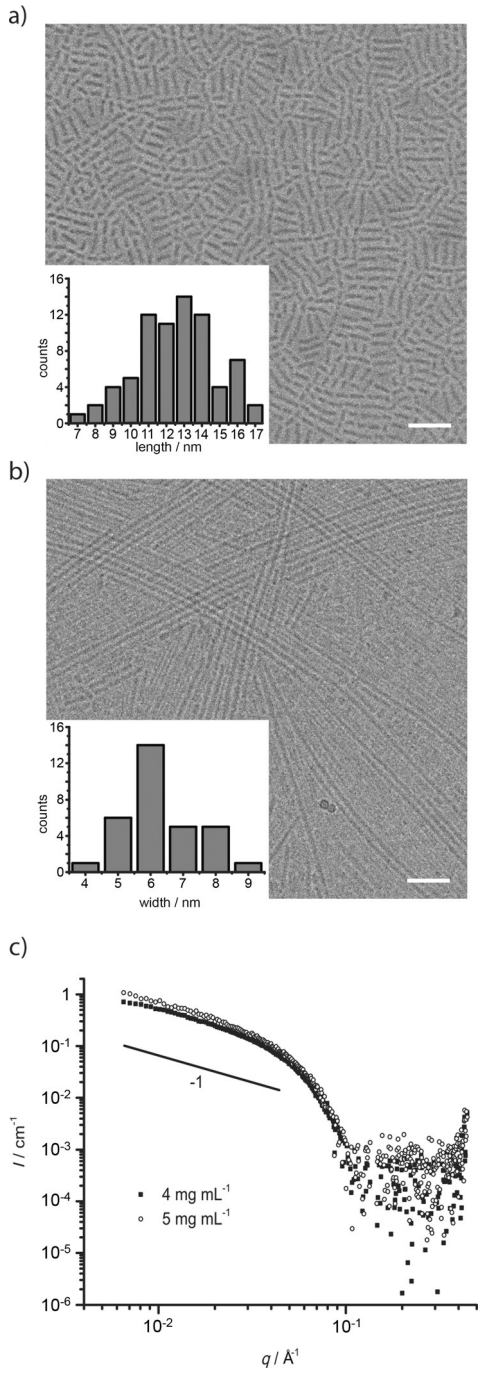

Figure 2. Cryo-TEM images of **1** in aqueous solution (1 wt%) after sonication: a) $t=0$, and b) $t=2$ weeks. Inset: Histograms of length (a) and width (b). Scale bar: a) 50 nm; b) 100 nm. c) Small-angle X-ray scattering profiles of squaramide fibers collected at a concentration of 4 and 5 mg mL^{-1}.

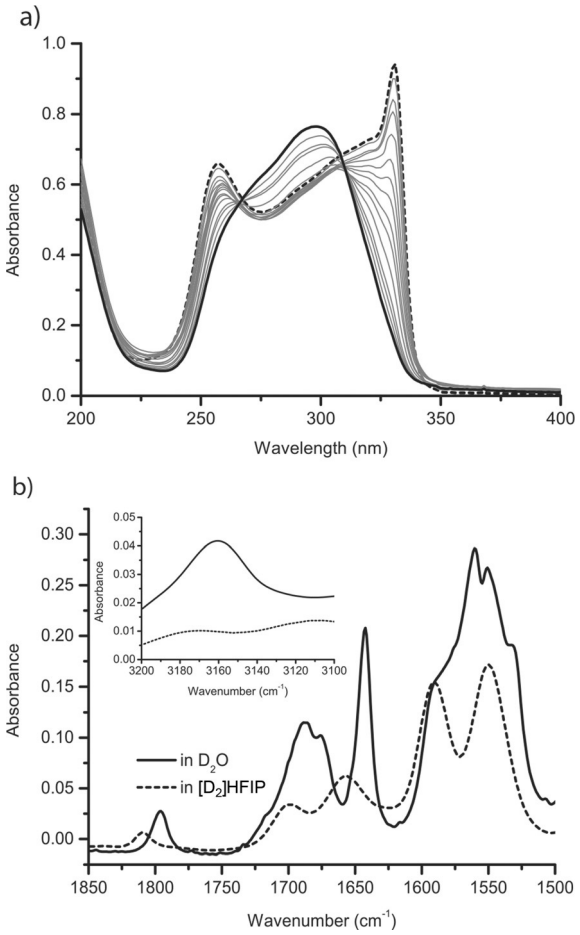

Figure 3. a) UV/Vis spectrum of **1** in water (0.005 wt%) as a function of HFIP concentration. b) IR spectrum recorded in the amide I region and amide II in D_2O and [D_2]HFIP. Inset: N–H and C–H stretch region.

one is defined for aromatic compounds. Experiments point to strong hydrogen bonding and computed geometric considerations demonstrate an increase in aromatic character within the squaramide unit due to supramolecular polymerization.

NICS-scan profiles,[15] a measurement of the magnetic shielding above and at the center of the ring, were computed on an axis passing though the center of the squaramide ring for monomers to pentamers to quantify the aromatic character upon oligomerization. The profiles for the individual squaramide units were negative overall and exhibited a minimum around 0.6 Å, consistent with an aromatic ring. Upon increasing oligomer length, the NICS values became more negative without a change in the shape of the curves, suggestive of increased aromaticity. In particular, the change in NICS at 0.6 Å from the ring plane (Figure 4b) when going from a monomer (−6.8) to the central monomer of a pentamer (−8.4), is in line with previous reports.[16] Additionally, the aromatic stabilization energy accounts for at least 30% of the total interaction energy in a squaramide pentamer (−85.6 kJ mol^{-1} out of −271.7 kJ mol^{-1} including BSSE correction) using a heterodimer of vinylogous amides that cannot exhibit aromaticity as a reference.

We further investigated the thermodynamic consequence of aromatic gain experimentally by measuring the critical aggregation concentration (CAC) using static light scattering (SLS). An order of magnitude lower CAC, corresponding to a free energy difference $\Delta\Delta G_{agg} = -5.25$ kJ mol^{-1}, was obtained for molecule **1** (7.94×10^{-6} M) in comparison to urea-based analogue **5** (7.41×10^{-5} M; see the Supporting Information) (Figure 5). These results are further supported

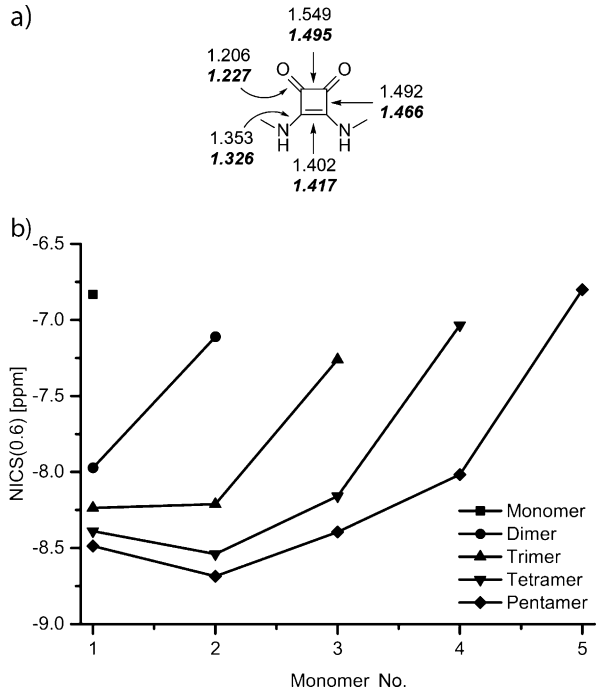

Figure 4. a) Geometric changes (computed at the M06-2X/6-311++G(d,p) level of theory) in *N*-methyl squaramide between an isolated monomer (normal text) and the central monomer in a pentamer (in bold italics). b) NICS values at a point 0.6 Å from the ring plane for an isolated monomer and each monomer in oligomers of length 2–5 (GIAO-M06-2X/6-311++G(d,p)).

by DFT calculations, where the interaction energy computed per hydrogen bond of urea oligomers was found to be smaller (−23.9 vs. −35.6 kJ mol^{-1} for pentamers) and does not increase as steeply with oligomer length (+18% vs. +30%). Intriguingly, a striking difference in the fiber morphology was found above the CAC of both molecules. Whereas **1** consistently formed long and stiff micron-sized fibers, short worm-like or spherical aggregates were obtained for **5**. Given the similarity of the hydrophilic and hydrophobic blocks, these results suggest that the coupling of aromatic gain and hydrogen-bonding in addition to the structural rigidity of the squaramide units act collectively to lower the critical aggregation concentration, and propagate the formation of high-aspect-ratio fibers in water.

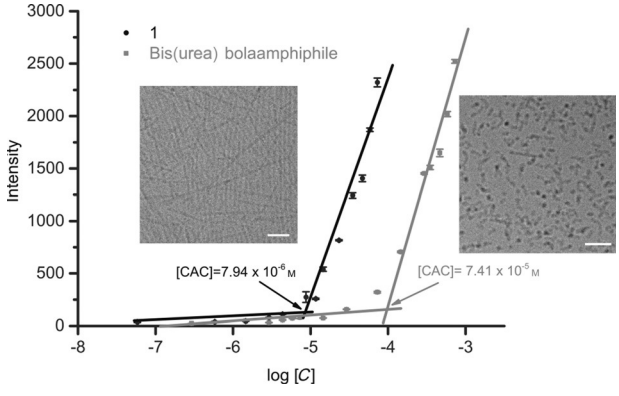

Figure 5. Scattered intensity (1000 s^{-1}) as a function of concentration, log[*C*], of **1** and **5** using static light scattering (SLS) experiments to determine the critical aggregation concentration (CAC). Representative cryo-TEM images: the image on the left belongs to **1** and the image on the right to **5**, showing fibrils in the case of **1** and worm-like or spherical aggregates in the case of **5**. Scale bar: 50 nm.

We find that the capacity of squaramides to couple hydrogen bonding and aromaticity facilitates the formation of robust supramolecular polymers. The gain in aromatic character upon assembly is demonstrated through bond length equalization, decreased NICS values, high aromatic stabilization (ASE) values, and increased thermodynamic stability of the resultant aggregates. These changes are in accordance with the geometric, magnetic, and energetic criteria used to describe aromaticity. Moreover, the aromatic gain is a significant component of the total interaction energy of squaramide-based supramolecular polymers, explaining the observed increase in thermodynamic stability relative to the monomers and to their urea counterparts. In summary, this self-tuning behavior between hydrogen bonding and aromaticity within the squaramide ring system cannot be achieved by other simple ditopic synthons, such as ureas or amides, commonly used to construct supramolecular polymers. Therefore, we anticipate that the information gained here can enrich the palette of hydrogen-bonding monomers used for supramolecular polymer assembly by implementing aromaticity as a design consideration.

Keywords: aromaticity · non-covalent interactions · self-assembly · squaramides · supramolecular polymers

How to cite: *Angew. Chem. Int. Ed.* **2015**, *54*, 10502–10506
Angew. Chem. **2015**, *127*, 10648–10652

[1] a) I. V. Alabugin, M. Manoharan, B. Breiner, F. D. Lewis, *J. Am. Chem. Soc.* **2003**, *125*, 9329–9342; b) C. F. Bernasconi, M. L. Ragains, S. Bhattacharya, *J. Am. Chem. Soc.* **2003**, *125*, 12328–12336; c) T. Bekele, M. H. Shah, J. Wolfer, C. J. Abraham, A. Weatherwax, T. Lectka, *J. Am. Chem. Soc.* **2006**, *128*, 1810–1811; d) D. J. Babinski, X. G. Bao, M. El Arba, B. Chen, D. A. Hrovat, W. T. Borden, D. E. Frantz, *J. Am. Chem. Soc.* **2012**, *134*, 16139–16142; e) M. R. Manaa, D. W. Sprehn, H. A. Ichord, *J. Am. Chem. Soc.* **2002**, *124*, 13990–13991; f) M. Manoharan, F. de Proft, P. Geerlings, *J. Org. Chem.* **2000**, *65*, 6132–6137.

[2] a) T. F. A. de Greef, M. M. J. Smulders, M. Wolffs, A. P. H. J. Schenning, R. P. Sijbesma, E. W. Meijer, *Chem. Rev.* **2009**, *109*, 5687–5754; b) T. Aida, E. W. Meijer, S. I. Stupp, *Science* **2012**, *335*, 813–817; c) N. Chebotareva, P. H. H. Bomans, P. M. Frederik, N. A. J. M. Sommerdijk, R. P. Sijbesma, *Chem. Commun.* **2005**, 4967–4969; d) C. M. A. Leenders, L. Albertazzi, T. Mes, M. M. E. Koenigs, A. R. A. Palmans, E. W. Meijer, *Chem. Commun.* **2013**, *49*, 1963–1965; e) G. Borzsonyi, R. L. Beingessner, T. Yamazaki, J. Y. Cho, A. J. Myles, M. Malac, R. Egerton, M. Kawasaki, K. Ishizuka, A. Kovalenko, H. Fenniri, *J. Am. Chem. Soc.* **2010**, *132*, 15136–15139; f) J. D. Hartgerink, E. Beniash, S. I. Stupp, *Science* **2001**, *294*, 1684–1688; g) E. Obert, M. Bellot, L. Bouteiller, F. Andrioletti, C. Lehen-Ferrenbach, F. Boue, *J. Am. Chem. Soc.* **2007**, *129*, 15601–15605; h) B. Rybtchinski, *ACS Nano* **2011**, *5*, 6791–6818; i) D. Görl, X. Zhang, F. Würthner, *Angew. Chem. Int. Ed.* **2012**, *51*, 6328–6348; *Angew. Chem.* **2012**, *124*, 6434–6455; j) J. van Esch, S. de Feyter, R. M. Kellogg, F. de Schryver, B. L. Feringa, *Chem. Eur. J.* **1997**, *3*, 1238–1243; k) J. van Esch, R. M. Kellogg, B. L. Feringa, *Tetrahedron Lett.* **1997**, *38*, 281–284.

[3] A. Kekulé, *Bull. Soc. Chem. Fr.* **1865**, *3*, 98.
[4] a) M. K. Cyrański, T. M. Krygowski, A. R. Katritzky, P. v. R. Schleyer, *J. Org. Chem.* **2002**, *67*, 1333 – 1338; b) K. K. Baldridge, J. S. Siegel, *J. Phys. Org. Chem.* **2004**, *17*, 740 – 742; c) R. M. Gomila, D. Quinonero, C. Rotger, C. Garau, A. Frontera, P. Ballester, A. Costa, P. M. Deya, *Org. Lett.* **2002**, *4*, 399 – 401; d) A. R. Katritzky, M. Karelson, S. Sild, T. M. Krygowski, K. Jug, *J. Org. Chem.* **1998**, *63*, 5228 – 5231.
[5] a) T. M. Krygowski, H. Szatylowicz, O. A. Stasyuk, J. Dominikowska, M. Palusiak, *Chem. Rev.* **2014**, *114*, 6383 – 6422; b) M. K. Cyrański, *Chem. Rev.* **2005**, *105*, 3773 – 3811; c) Z. F. Chen, C. S. Wannere, C. Corminboeuf, R. Puchta, P. v. R. Schleyer, *Chem. Rev.* **2005**, *105*, 3842 – 3888.
[6] P. v. R. Schleyer, C. Maerker, A. Dransfeld, H. J. Jiao, N. J. R. V. Hommes, *J. Am. Chem. Soc.* **1996**, *118*, 6317 – 6318.
[7] T. M. Krygowski, *J. Chem. Inf. Comput. Sci.* **1993**, *33*, 70 – 78.
[8] J. I. Wu, J. E. Jackson, P. v. R. Schleyer, *J. Am. Chem. Soc.* **2014**, *136*, 13526 – 13529.
[9] a) F. R. Wurm, H. A. Klok, *Chem. Soc. Rev.* **2013**, *42*, 8220 – 8236; b) R. I. Storer, C. Aciro, L. H. Jones, *Chem. Soc. Rev.* **2011**, *40*, 2330 – 2346.
[10] M. C. Rotger, M. N. Pina, A. Frontera, G. Martorell, P. Ballester, P. M. Deya, A. Costa, *J. Org. Chem.* **2004**, *69*, 2302 – 2308.
[11] R. Prohens, A. Portell, C. Puigjaner, R. Barbas, X. Alcobe, M. Font-Bardia, S. Tomas, *CrystEngComm* **2012**, *14*, 5745 – 5748.
[12] G. Gilli, V. Bertolasi, P. Gilli, V. Ferretti, *Acta Crystallogr. Sect. B* **2001**, *57*, 859 – 865.
[13] a) G. Ambrosi, M. Formica, V. Fusi, L. Giorgi, A. Guerri, M. Micheloni, P. Paoli, R. Pontellini, P. Rossi, *Chem. Eur. J.* **2007**, *13*, 702 – 712; b) N. Busschaert, I. L. Kirby, S. Young, S. J. Coles, P. N. Horton, M. E. Light, P. A. Gale, *Angew. Chem. Int. Ed.* **2012**, *51*, 4426 – 4430; *Angew. Chem.* **2012**, *124*, 4502 – 4506; c) A. Rostami, G. Guerin, M. S. Taylor, *Macromolecules* **2013**, *46*, 6439 – 6450.
[14] L. Sobczyk, S. J. Grabowski, T. M. Krygowski, *Chem. Rev.* **2005**, *105*, 3513 – 3560.
[15] A. Stanger, *J. Org. Chem.* **2006**, *71*, 883 – 893.
[16] D. Quiñonero, R. Prohens, C. Garau, A. Frontera, P. Ballester, A. Costa, P. M. Deyà, *Chem. Phys. Lett.* **2002**, *351*, 115 – 120.

Received: April 28, 2015
Published online: July 14, 2015

